

**FUNCTIONAL ASSESSMENT OF SUBURETHRAL TISSUE BIOMECHANICS
USING STANDARDIZED STRAIN ELASTOGRAPHY IN WOMEN WITH STRESS
URINARY INCONTINENCE**

Lóránt Csákány, M.D.

PhD Thesis

Szeged

2026

University of Szeged
Albert Szent-Györgyi Medical School
Doctoral School of Clinical Medicine

**FUNCTIONAL ASSESSMENT OF SUBURETHRAL TISSUE BIOMECHANICS
USING STANDARDIZED STRAIN ELASTOGRAPHY IN WOMEN WITH STRESS
URINARY INCONTINENCE**

PhD Thesis

Lóránt Csákány, M.D.

Supervisors

Norbert Pásztor, M.D., PhD, habil.
Prof. Gábor Németh, M.D., PhD, habil.

Szeged
2026

TABLE OF CONTENTS

PUBLICATIONS	1
LIST OF ABBREVIATIONS	2
1. INTRODUCTION	3
1.1. Pathophysiology of stress urinary incontinence	3
1.2. Etiological factors contributing to pelvic floor biomechanical weakening.....	4
1.3. Anatomical and biomechanical context of suburethral support	4
1.4. Diagnostic gap in conventional pelvic floor imaging.....	6
1.5. Elastography in pelvic floor imaging: principles and techniques	6
1.5.1. Strain elastography (SE)	7
1.5.2. Shear wave elastography (SWE)	8
2. OBJECTIVES.....	8
2.1. Aim of the thesis.....	8
2.2. Study design	8
2.3. Specific objectives.....	9
3. MATERIALS AND METHODS	9
3.1. Original prospective cohort study	9
3.1.1. Study participants	9
3.1.2. Inclusion criteria	10
3.1.3. Exclusion criteria	10
3.1.4. Sample size and power analysis	11
3.1.5. Introital sonography	11
3.1.6. Strain elastography protocol	12
3.1.7. Placement of regions of interest (ROIs)	13
3.1.8. Statistical evaluation.....	14
3.1.9. Trial registration	15
3.2. Methodology of the structured literature review	15
3.2.1. Objective.....	15
3.2.2. Search strategy	15
3.2.3. Eligibility criteria and data synthesis.....	15

4. RESULTS.....	17
4.1. Results of the original prospective cohort study	17
4.1.1. Demographic and clinical characteristics.....	17
4.1.2. Strain elastography measurements.....	17
4.1.3. Reproducibility of strain elastography measurements	19
4.1.4. Diagnostic performance of strain elastography for stress urinary incontinence	21
4.2. Results of the structured literature review	24
5. DISCUSSION.....	26
5.1. Interpretation of the main findings	26
5.2. Comparison with previous strain elastography studies	27
5.3. Reproducibility and methodological robustness	27
5.4. Obstetric contributions to suburethral biomechanical impairment	28
5.5. Relationship of the present findings to previous elastography and biomechanical research.....	28
5.6. Limitations and future perspectives.....	30
5.7. Clinical implications.....	30
6. CONCLUSION	31
ACKNOWLEDGEMENTS	32
REFERENCES.....	33
SUPPLEMENTARY MATERIALS.....	38

PUBLICATIONS

Publications related to the thesis:

1. **Csákány L**, Kozinszky Z, Kovács F, Krajczár S, Várbíró Sz, Keresztúri A, Németh G, Surányi A, Pásztor N. *Evaluation of Suburethral Tissue Elasticity Using Strain Elastography in Women with Stress Urinary Incontinence*. JCM. 2025 Aug 8;14(16):5617. doi:10.3390/jcm14165617
Original article
SJR: Q1; IF: 2.9
2. **Csákány L**, Surányi A, Kovács F, Várbíró Sz, Németh G, Keresztúri A, Pásztor N. *Strain Elastography in Urogynecology: Functional Imaging in Stress Urinary Incontinence*. Women. 2025 Dec;5(4):48. doi:10.3390/women5040048
Review article
IF: 1.6
3. **Csákány L**, Pásztor N, Németh G, Várbíró Sz, Surányi A. *Identifying Weak Points of the Pelvic Floor by Sonoelastography in Stress Urinary Incontinence. Ultrasound in Obstetrics & Gynecology*, 64(Suppl. 1): 97–98 (2024). doi: 10.1002/uog.27990
Conference abstract

Σ IF: 4.5

LIST OF ABBREVIATIONS

AL = adipose layer

AUC = area under the curve

B-mode = brightness-mode ultrasonography

BMI = body mass index

EUO = external urethral orifice

FN = false negative

FP = false positive

ICC = intraclass correlation coefficient

ICS = International Continence Society

ISD = intrinsic sphincter deficiency

IUS = internal urethral sphincter

IUO = internal urethral orifice

kPa = kilopascal

MANOVA = multivariate analysis of variance

Meas = measurement

MRI = magnetic resonance imaging

MU = midurethra

N = number of subjects

NPV = negative predictive value

NS = not significant

PPV = positive predictive value

ROI = region of interest

ROC = receiver operating characteristic

SD = standard deviation

SE = strain elastography

SUI = stress urinary incontinence

SWE = shear wave elastography

TN = true negative

TP = true positive

1. INTRODUCTION

Stress urinary incontinence (SUI) is one of the most common chronic pelvic floor disorders in women and represents a major cause of physical limitation, psychosocial distress, and reduced quality of life [1, 2]. Lifetime prevalence rates exceed 60%, with the greatest burden observed among parous, postmenopausal, and overweight women, highlighting the considerable public health and socioeconomic impact of this condition [3]. Although SUI is not life-threatening, it significantly affects daily activities, social participation, and overall well-being, and is associated with substantial healthcare utilization worldwide [1–3].

Among the different subtypes of urinary incontinence, SUI is the most prevalent, affecting up to 25% of women globally [2]. The International Continence Society (ICS) defines SUI as the involuntary loss of urine during physical exertion or activities associated with increased intra-abdominal pressure, such as coughing, sneezing, or exercise [1, 2]. From a functional perspective, continence failure occurs when increases in intra-abdominal pressure are no longer adequately counterbalanced by urethral resistance. Importantly, this process reflects impaired pelvic floor support and ineffective pressure transmission rather than isolated dysfunction of the urethra alone [1, 4].

1.1. Pathophysiology of stress urinary incontinence

SUI arises when the mechanical forces required to maintain urethral closure are no longer adequately supported by a structurally intact and biomechanically competent suburethral support system capable of efficient load transfer [1, 2]. Contemporary concepts increasingly characterize SUI as a disorder of impaired pelvic floor biomechanics, in which continence failure results primarily from reduced tissue stiffness, altered deformation behavior, and impaired transmission of intra-abdominal pressure rather than urethral descent alone [1, 2, 5, 6].

A key pathophysiological feature of SUI is urethral hypermobility, most commonly associated with compromised suburethral support rather than isolated intrinsic sphincter deficiency (ISD) [1, 2, 5]. Disruption of the structural and biomechanical integrity of paraurethral connective tissues and their supporting structures—resulting from extracellular matrix remodeling, altered collagen architecture, neuromuscular injury, or reduced tissue viscoelasticity—leads to diminished suburethral support capacity. Consequently, load transmission becomes impaired, tissue deformation increases, and urethral closure pressure decreases, ultimately resulting in stress-induced urinary leakage [4, 7–11].

1.2. Etiological factors contributing to pelvic floor biomechanical weakening

The biomechanical deterioration underlying SUI is multifactorial and reflects the combined effects of obstetric trauma, neuromuscular injury, hormonal alterations, metabolic factors, and chronic mechanical loading [1, 2, 5, 7, 12]. Vaginal childbirth is widely regarded as the most prominent etiological factor, as it may simultaneously compromise the muscular, fascial, and neural components of the continence mechanism [7, 12, 13]. Additional contributors, including advancing age, estrogen deficiency, increased body mass index (BMI), and prior pelvic surgery, further promote connective tissue softening and diminish the load-bearing capacity of the pelvic floor [1, 2, 5, 7, 14].

Obesity is associated with chronically elevated intra-abdominal pressure, resulting in increased baseline and dynamic loading of the pelvic floor. Urodynamic investigations have consistently demonstrated higher intravesical pressures in obese women, supporting a direct biomechanical relationship between sustained pelvic floor strain and the development of SUI [2, 14]. Lifestyle-related factors such as chronic coughing, smoking, and repetitive heavy lifting impose cumulative mechanical stress and contribute to progressive tissue fatigue within the pelvic floor [2, 6, 15]. In a smaller subset of patients, continence failure is predominantly driven by intrinsic sphincter deficiency (ISD), most commonly linked to neuromuscular injury, pelvic radiotherapy, or previous anti-incontinence surgery [2].

Taken together, these etiological processes lead to a distinct biomechanical profile with reduced tissue stiffness, impaired adaptive stiffening under load, and excessive deformation of the suburethral support platform. Importantly, many of these alterations primarily affect tissue mechanical properties rather than gross anatomical displacement, highlighting the need for functional biomechanical assessment methods.

1.3. Anatomical and biomechanical context of suburethral support

Over the past three decades, the conceptual understanding of SUI has evolved from predominantly static anatomical explanations toward dynamic biomechanical models of continence. A major conceptual milestone in this transition was the suburethral hammock hypothesis proposed by John O. L. DeLancey (**Figure 1**), which posits that effective urethral closure during increases in intra-abdominal pressure depends primarily on the stiffness, integrity, and load-bearing capacity of the suburethral support system rather than on urethral position alone. According to this model, continence is achieved through compression of the urethra against a functionally integrated fibromuscular support layer composed of the anterior vaginal wall, endopelvic fascia, perineal membrane, arcus tendineus fasciae pelvis, and the

levator ani muscle complex. Collectively, these structures form a dynamic support platform that enables efficient load transfer and coordinated mechanical resistance during stress, thereby facilitating urethral closure [5, 7, 12, 13].

Within this framework, the midurethral segment represents a key biomechanical region in which fascial anchorage and active muscular stabilization interact to counteract increases in intra-abdominal pressure. When the stiffness, structural continuity, or viscoelastic properties of this support layer are compromised, pressure transmission becomes ineffective, leading to urethral hypermobility and subsequent continence failure. From this perspective, urinary continence can be understood as a stiffness-dependent, load-transfer-mediated musculoelastic function rather than a purely positional or static anatomical phenomenon [5, 6, 9, 16].

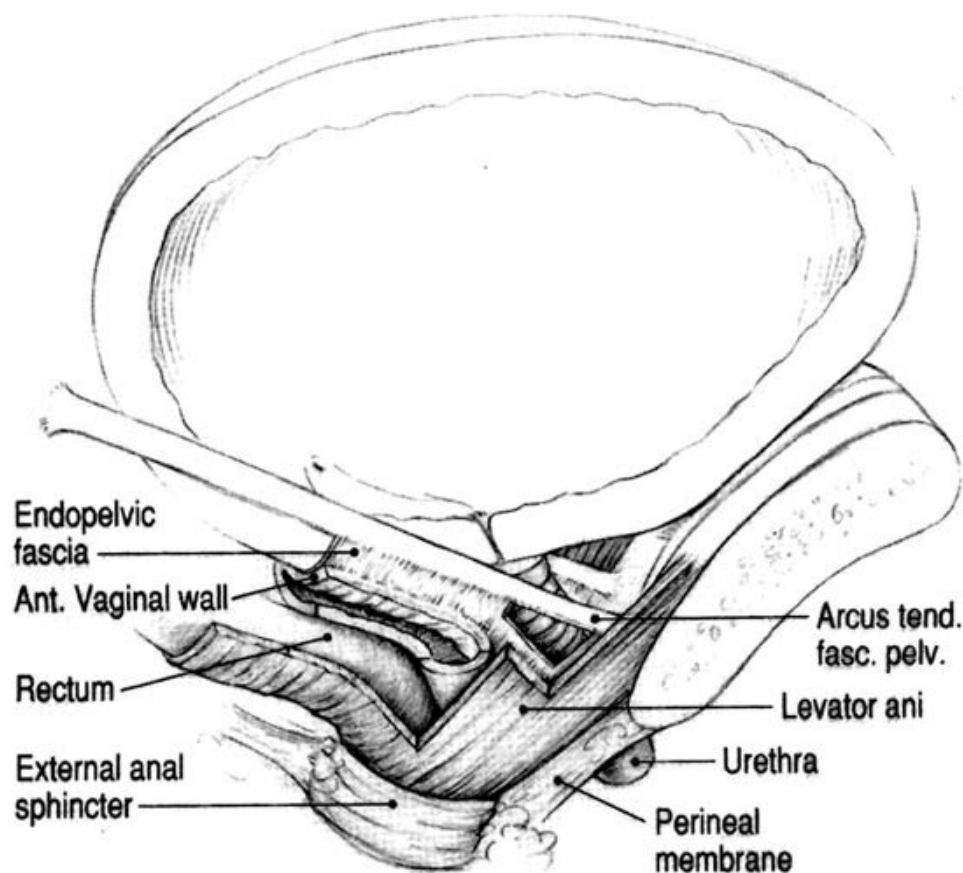


Figure 1. Anatomical structures involved in urethral support according to the hammock hypothesis. The urethra is supported by a functionally integrated suburethral layer composed of the anterior vaginal wall and the endopelvic fascia. This supportive layer provides structural stability through its lateral suspension to the pelvic sidewall via the arcus tendineus fasciae pelvis, a dense fibrous band extending between the pubic bone and the ischial spine. At the level of the midurethra, the endopelvic fascia is supported medially by the levator ani muscle complex, forming a coordinated fibromuscular–fascial system that enables effective load transfer and tensioning during increases in intra-abdominal pressure. Together, these structures create a dynamic, stiffness-dependent “hammock” that facilitates urethral compression and stability, thereby contributing to the maintenance of urinary continence [5].

(Adapted from: DeLancey JO. Structural Support of the Urethra as It Relates to Stress Urinary Incontinence: The Hammock Hypothesis. Am J Obstet Gynecol. 1994;170:1713–1720.)

1.4. Diagnostic gap in conventional pelvic floor imaging

Despite substantial advances in urogynecologic imaging, currently available imaging modalities remain primarily focused on anatomical configuration and kinematic assessment [17]. Introital and transperineal ultrasound are widely used to evaluate urethral mobility, bladder neck descent, and pelvic organ prolapse; however, these techniques do not provide direct information on the mechanical competence, stiffness, or load-bearing capacity of periurethral tissues [12, 17]. Similarly, three- and four-dimensional ultrasound and magnetic resonance imaging (MRI) allow detailed visualization of structural alterations and spatial relationships, yet they do not quantify tissue deformation behavior or functional load transfer during physiological loading conditions [8, 18, 19].

This limitation represents an important diagnostic gap, as contemporary biomechanical concepts of continence increasingly emphasize tissue stiffness, viscoelastic behavior, and effective force transmission as key functional determinants. Consequently, there is a clear need for in vivo functional imaging methods capable of evaluating the mechanical properties of the suburethral support system rather than relying solely on static anatomical assessment.

1.5. Elastography in pelvic floor imaging: principles and techniques

Elastography emerged in the early 1990s as an ultrasound-based imaging modality capable of visualizing tissue deformation in response to externally or internally applied mechanical stress. It provides functional insight into biomechanical tissue properties such as stiffness and elasticity, extending beyond the purely morphological information obtained from conventional grayscale ultrasound imaging [20]. In contrast to standard B-mode ultrasound, which primarily depicts anatomical structures and spatial relationships, elastography adds a functional dimension by characterizing tissue behavior under load—a property that is fundamental to pelvic floor physiology and the maintenance of urinary continence [20–22].

In the context of pelvic floor assessment, urinary continence depends not only on anatomical integrity but also on tissue stiffness, compliance, and effective force transmission within the suburethral support system. Elastography therefore represents both a conceptual and methodological extension of traditional pelvic floor imaging, as it directly aligns with contemporary biomechanical models of SUI pathophysiology. By visualizing strain distribution or shear-wave propagation within tissues, elastographic techniques enable qualitative, semi-quantitative, or quantitative evaluation of tissue elasticity—parameters that cannot be assessed using grayscale ultrasound alone but are essential for the functional characterization of suburethral support structures [21–23].

Currently, two principal elastographic techniques are used in clinical practice and research applications: strain elastography (SE) and shear wave elastography (SWE) [21, 23].

1.5.1. Strain elastography (SE)

SE assesses relative tissue deformation induced by gentle external compression, with strain patterns displayed as color-coded maps superimposed on B-mode ultrasound images (**Figure 2**). Because the magnitude of the applied stress is not directly measured, SE provides relative rather than absolute estimates of tissue stiffness and does not allow direct calculation of material properties such as Young's modulus. Instead, it enables qualitative and semi-quantitative assessment of tissue stiffness based on the degree of deformation relative to surrounding tissues [21, 23].

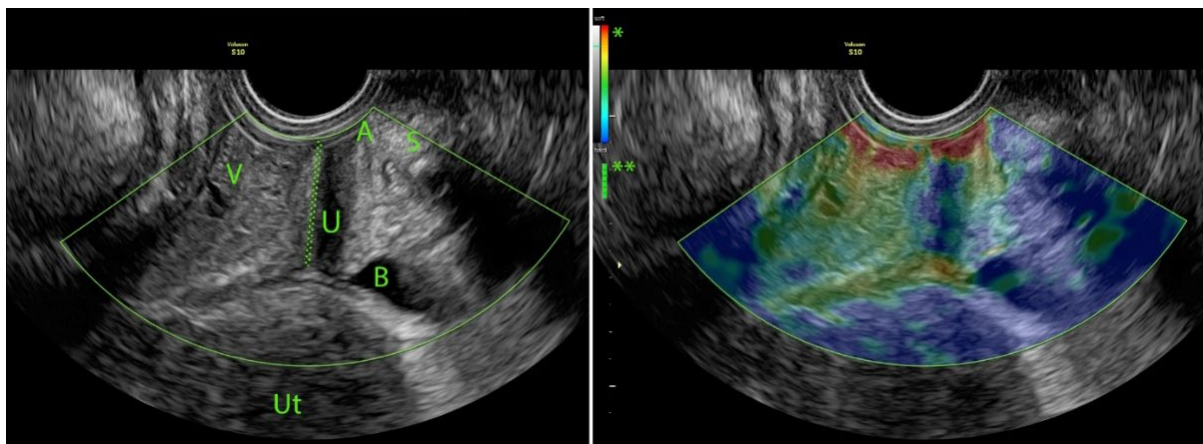


Figure 2. Introital B-mode ultrasound image (left) combined with strain elastography (right) demonstrating suburethral tissue elasticity and adjacent supporting structures.

The elastographic map is overlaid on the grayscale image, enabling spatial correlation between anatomical landmarks and relative tissue stiffness. Tissue stiffness is visualized using a color-coded strain scale (red/yellow = softer tissue, blue/green = stiffer tissue). The built-in strain indicator bar provides real-time feedback to ensure optimal compression during image acquisition.

Legend: V: vagina; A: periurethral adipose layer; S: symphysis pubis; U: urethra; dotted line: suburethral supportive layer; B: bladder; Ut: uterus; *: color scale indicating tissue stiffness (soft → hard); **: strain indicator demonstrating optimal compression (score 6/6).

Ultrasound system: GE Voluson S10 (BT18) equipped with a RIC5-9A-RS transvaginal transducer (GE HealthCare, Tiefenbach, Austria).

Accurate and reproducible SE assessment therefore requires rigorous methodological standardization. In urogynecological applications, this includes the use of anatomically predefined regions of interest (ROIs) and normalization against an internal reference tissue within the same imaging field. This approach reduces variability related to probe pressure, tissue depth, and inter-individual anatomical differences. Within such a standardized

framework, SE enables localized functional assessment of tissue deformation and relative stiffness in the suburethral and paraurethral support structures, providing biomechanical information that complements conventional morphological imaging [21, 23, 24].

1.5.2. Shear wave elastography (SWE)

SWE is based on the generation of shear waves induced by acoustic radiation force, whose propagation velocity can be translated into absolute quantitative measures of tissue stiffness, most commonly expressed as Young's modulus in kilopascals (kPa). Because SWE does not rely on externally applied manual compression, it minimizes operator-dependent variability and offers improved measurement objectivity and reproducibility compared with strain-based elastographic techniques [23, 25].

Despite these advantages, SE was selected as the primary elastographic technique in this study. This decision was based on several methodological and practical considerations. SE is widely available on conventional ultrasound systems and can be readily integrated into routine urogynecological introital or transvaginal pelvic floor imaging, facilitating its use in everyday clinical practice.

2. OBJECTIVES

2.1. Aim of the thesis

SUI is increasingly recognized as a disorder of impaired pelvic floor biomechanics affecting the suburethral support system. However, elastographic evaluation of this region in women with SUI remains relatively underexplored in clinical imaging studies.

The objective of this thesis was to characterize the biomechanical properties of the suburethral support system in women with clinically confirmed pure SUI using standardized introital SE, and to evaluate the feasibility, reproducibility, and diagnostic relevance of this imaging approach.

2.2. Study design

To achieve these objectives, the thesis comprised two complementary research components:

- I. Prospective observational cohort study:** comparison of women with pure SUI and continent controls using standardized introital ultrasound and SE with anatomically predefined ROIs and internal reference-tissue normalization.

II. Structured literature review: qualitative analysis of elastography applications in pelvic floor disorders associated with SUI, with interpretation of the findings within the context of the international literature.

2.3. Specific objectives

1) Protocol development

To develop a standardized and reproducible introital SE acquisition and analysis protocol using anatomically predefined ROIs and internal reference-tissue normalization.

2) Biomechanical characterization

To evaluate level-specific differences in suburethral tissue deformability at the levels of the internal urethral orifice (IUO), the midurethra (MU), and the external urethral orifice (EUO).

3) Diagnostic evaluation

To assess the diagnostic performance of SE-derived parameters across predefined ROIs using receiver operating characteristic (ROC) curve analysis and to identify the most informative suburethral level.

4) Measurement reliability

To evaluate the reproducibility and internal consistency of repeated SE measurements at each ROI using intraclass correlation coefficients (ICC) and Cronbach's alpha.

5) Literature synthesis

To conduct a structured literature review of elastography applications in pelvic floor disorders associated with SUI and to interpret the findings in the context of the international literature.

3. MATERIALS AND METHODS

3.1. Original prospective cohort study

3.1.1. Study participants

Based on methodological considerations derived from the literature review, a prospective observational cohort study was designed to evaluate the biomechanical properties of suburethral tissues using SE. The study was conducted between 16 August 2024 and 1 January 2025 at the Department of Obstetrics and Gynecology, Albert Szent-Györgyi Medical School, University of Szeged, Hungary. Consecutive women referred for urogynecological evaluation were assessed by an obstetrician–gynecologist with more than five years of dedicated clinical

experience in urogynecology. Twenty women with clinically confirmed pure SUI were enrolled and compared with twenty healthy continent women serving as controls.

3.1.2. Inclusion criteria

Women were eligible for inclusion if they met all of the following criteria:

- age ≥ 35 years;
- ability to provide written informed consent;
- for the SUI group:
 - symptoms of involuntary urine leakage during physical exertion, coughing, or sneezing;
 - a positive cough stress test performed with a comfortably full bladder (≥ 200 mL);
- for the control group:
 - absence of current or prior symptoms of urinary incontinence;
 - a negative cough stress test;
- ability to undergo introital ultrasound examination with adequate image quality.

3.1.3. Exclusion criteria

Women were excluded from participation if they met any of the following criteria:

- pelvic organ prolapse in any compartment;
- mixed urinary incontinence;
- prior vaginal reconstructive or urethral surgery;
- history of bladder augmentation;
- post-void residual volume > 150 mL;
- current smoking;
- known connective tissue disorders;
- technically inadequate ultrasound imaging due to body habitus;
- hormonal therapy within the previous 12 months;
- untreated urinary tract infection;
- current malignancy;
- severe psychiatric illness;
- pregnancy.

3.1.4. Sample size and power analysis

Sample size estimation was performed before study initiation using G*Power software (Heinrich Heine University Düsseldorf, Düsseldorf, Germany). The purpose of this analysis was to determine the number of participants required for this pilot study evaluating the diagnostic applicability of SE in women with SUI. As no previously published effect size estimates are available for paraurethral SE parameters in SUI populations, a moderate standardized effect size (Cohen's $d = 0.7$) was predefined, consistent with methodological assumptions commonly applied in exploratory biomechanical imaging research [26].

Assuming a two-sided significance level of $\alpha = 0.05$ and statistical power of 80% ($\beta = 0.20$), the calculation indicated that a sample size of 20 participants per group was sufficient to detect statistically significant differences between women with pure SUI and continent controls [26].

3.1.5. Introital sonography

Introital ultrasound was performed with the transducer placed at the level of the EUO and aligned parallel to the longitudinal body axis. All measurements were obtained with the participant in the supine position, with the hips abducted and the knees slightly flexed, a standardized posture facilitating relaxation of the pelvic floor musculature. Participants were asked to empty their bladder prior to image acquisition to ensure uniform baseline conditions.

Minimal transducer pressure was applied to avoid artificial compression of suburethral tissues, bladder neck displacement, and interference with physiological urethral mobility and pelvic floor dynamics [27].

Midsagittal B-mode ultrasound images were obtained both at rest and during the Valsalva maneuver. In this plane, the urethra was visualized in a retropubic position, approximately perpendicular to the pelvic floor. The imaging field included the entire urethra from the bladder neck to the external urethral meatus, as well as the pubic symphysis and the anterior vaginal wall, enabling standardized assessment of urethral funneling and mobility [19, 27, 28].

Bladder neck mobility was quantified by measuring the vertical displacement of the bladder neck relative to the inferoposterior margin of the pubic symphysis. A caudal displacement >10 mm during the Valsalva maneuver was considered indicative of urethral hypermobility according to established diagnostic criteria [29].

3.1.6. Strain elastography protocol

SE was used to assess relative suburethral tissue stiffness. This technique is based on controlled tissue deformation induced by externally applied compression, whereby softer tissues deform more than stiffer tissues under comparable loading conditions [21, 30, 31].

SE acquisition was performed using a transvaginal ultrasound transducer. Gentle manual compression was applied to generate strain within the suburethral tissues, following established methodological recommendations. To minimize signal artifacts and avoid distortion caused by precompression, only light and uniform probe contact with the vaginal wall was maintained throughout the examination.

During image acquisition, the transducer was maintained in a stable position for at least 5 seconds with minimal axial or lateral movement, in accordance with previously described protocols [32]. Tissue deformation was assessed by tracking alterations in speckle patterns before and after compression. A two-dimensional B-mode image and the corresponding strain elastogram were displayed simultaneously using a dual-panel visualization mode (**Figure 3**).

Strain elastograms were displayed in real time as color-coded maps (**Figure 2**). Compression quality was continuously monitored using the ultrasound system's built-in strain indicator bar. All measurements were obtained under resting conditions to avoid potential confounding effects of pelvic floor contraction or straining.

For standardized assessment of suburethral tissue elasticity, circular ROIs with a fixed diameter of 5 mm were manually positioned at predefined anatomical locations between the urethra and the anterior vaginal wall. This approach enabled systematic, level-specific evaluation of tissue elasticity along the longitudinal axis of the urethra.

Image quality was assessed using a standardized six-point compression quality scale. Only elastograms achieving scores of 5 or 6 were included in the final analysis.

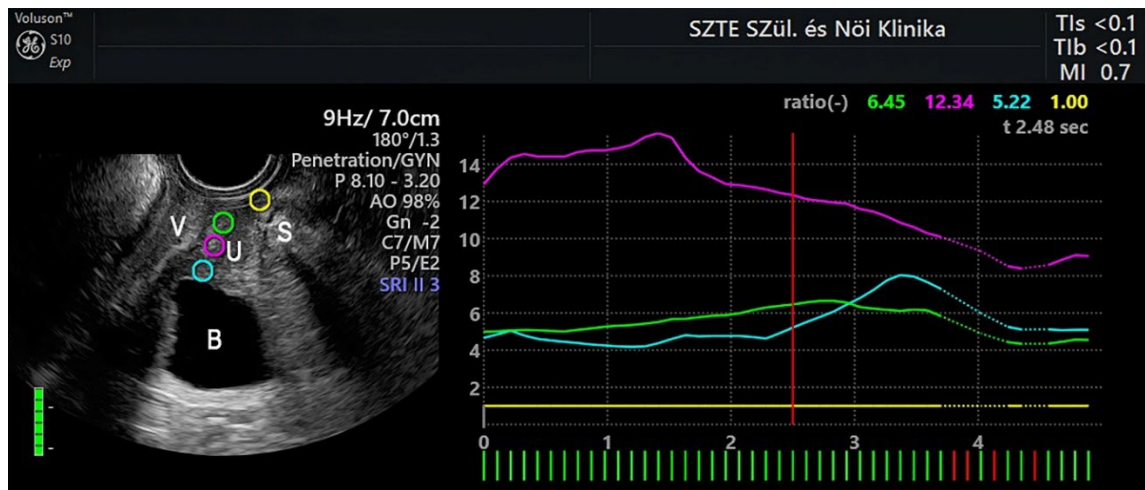


Figure 3. Anatomical locations of the regions of interest (ROIs) used for strain elastography measurements.

Legend: V: vagina; U: urethra; B: bladder; S: symphysis pubis. The blue ROI represents the suburethral tissues at the level of the internal urethral orifice (IUO). The purple ROI indicates the endopelvic fascia at the level of the midurethra (MU). The green ROI marks the suburethral tissues at the level of the external urethral orifice (EUO). The yellow ROI represents periurethral adipose tissue (AL) located between the EUO and the symphysis pubis and serves as an internal reference region for normalization of strain values.

The strain–time curve illustrates the measurement process, and the vertical red line marks the time point used for strain ratio calculation. The standardized six-point strain indicator reflects elastographic signal quality and the adequacy of transducer compression.

3.1.7. Placement of regions of interest (ROIs)

ROIs were defined based on clearly identifiable anatomical landmarks and standardized color coding to ensure consistent placement across examinations (**Figure 3**).

3.1.7.1. Yellow ROI: Adipose layer (AL)

The yellow ROI was placed within the periurethral adipose tissue between the EUO and the pubic symphysis. This region served as an internal reference tissue due to its high adipocyte content, low intrinsic stiffness, and lack of direct involvement in urethral support mechanisms, providing a stable reference for relative strain normalization [33, 34].

3.1.7.2. Blue ROI: Internal urethral orifice (IUO) level

The blue ROI was positioned in the suburethral region at the level of the IUO, anatomically corresponding to the bladder neck. This region contains smooth muscle fibers continuous with the detrusor muscle and contributes to the internal urethral sphincter (IUS) complex, playing an important role in urethral closure during increases in intra-abdominal pressure [7, 33, 35].

3.1.7.3. Purple ROI: Midurethral (MU) level

The purple ROI was defined at the midurethral level at the interface between the urethral wall and the adjacent endopelvic connective tissue. This region represents a key biomechanical support zone where the levator ani muscle and the endopelvic fascia interact to facilitate effective load transmission and urethral compression in accordance with the hammock hypothesis [6, 7, 19, 33, 35].

3.1.7.4. Green ROI: External urethral orifice (EUO) level

The green ROI was placed at the distal urethral segment between the EUO and the anterior vaginal wall. This region mainly consists of loose connective tissue and functions primarily as a distal transitional and anchoring zone [7, 33, 35].

ROI placement was standardized across all participants to enable reproducible level-specific assessment of tissue elasticity at the three predefined suburethral levels. For repeatability assessment, five consecutive strain measurements were obtained at each ROI, and peak strain values were recorded for statistical analysis.

In the present cohort, the mean urethral length was 30.8 mm, within the reported physiological range of 19–45 mm for the adult female urethra [36].

3.1.8. Statistical evaluation

Statistical analyses were performed using R software (version 4.2.1) [37]. Categorical variables were reported as absolute frequencies and percentages (n, %), whereas continuous variables were expressed as mean \pm standard deviation (SD). To further characterize the distribution of ultrasound-derived measurements within the SUI and control groups, skewness and kurtosis were calculated. Normality of SE-derived variables was assessed using the Kolmogorov–Smirnov test.

Between-group comparisons were performed using the chi-square (χ^2) test for categorical variables, the independent-samples t-test for normally distributed continuous variables, and the Wilcoxon rank-sum test for non-normally distributed data.

Measurement reliability was evaluated using ICCs and Cronbach's alpha [38]. Values > 0.90 were interpreted as indicating excellent reproducibility and internal consistency [39].

Differences in mean SE values across repeated measurements at each ROI were analyzed using multivariate analysis of variance (MANOVA) with adjustment for age and BMI at the

IUO, MU, and EUO levels. Overall model significance was assessed using Wilks' lambda, and homogeneity of variances was tested using Levene's test. When significant effects were detected, post hoc pairwise comparisons were performed using the Games–Howell procedure.

All statistical tests were two-sided, and $p < 0.05$ was considered statistically significant.

Diagnostic performance was evaluated using ROC curve analysis for each ROI, with calculation of the corresponding area under the curve (AUC) [38]. AUC values >0.90 were interpreted as indicating strong discriminatory performance [40]. Additional diagnostic indices—including sensitivity, specificity, positive predictive value (PPV), negative predictive value (NPV), and the F1 score [41]—were calculated to provide a comprehensive assessment of the classification performance of SE.

3.1.9. Trial registration

The study was registered at ClinicalTrials.gov under the title “*Elastographic Assessment of Suburethral Tissue in Continent and Incontinent Women (SE-inc1)*” (ClinicalTrials.gov identifier: NCT06933407). The trial was registered on 16 August 2024 and accessed on 5 August 2025.

3.2. Methodology of the structured literature review

3.2.1. Objective

This review synthesized the available scientific evidence on the application of SE in pelvic floor disorders associated with SUI, focusing on reported diagnostic findings, biomechanical interpretations, and methodological approaches.

3.2.2. Search strategy

A structured PubMed search was conducted covering publications from January 2000 to October 2025. The following predefined keyword combinations were used:

- “strain elastography” AND “female stress urinary incontinence”
- “stress incontinence” AND “elastography”

The search was limited to peer-reviewed articles published in English.

3.2.3. Eligibility criteria and data synthesis

Studies were eligible if they included adult female populations (≥ 18 years) and reported elastographic assessment of periurethral or pelvic floor tissues relevant to SUI. Studies focusing

on male populations, non-elastographic imaging modalities, or unrelated pelvic floor conditions were excluded.

After screening titles and abstracts, the full texts of potentially relevant articles were assessed for eligibility.

Given the limited number of SE-specific clinical studies and the substantial heterogeneity in study designs, imaging techniques, anatomical targets, and reported outcome parameters, quantitative synthesis was not feasible. Therefore, a structured qualitative evaluation was performed, focusing on imaging methodology, ROI definition and placement, biomechanical interpretation of elastographic parameters, and reported clinical implications.

To provide methodological and biomechanical context, the review also included selected studies using SWE, relevant international guidelines, and key biomechanical publications addressing urethral support mechanisms and pelvic floor function. These sources were incorporated to ensure conceptual coherence, terminological consistency, and alignment with established diagnostic frameworks of the ICS.

4. RESULTS

4.1. Results of the original prospective cohort study

4.1.1. Demographic and clinical characteristics

Participant characteristics are summarized in **Table 1**. Compared with continent controls, women with SUI had significantly higher body weight and BMI. In contrast, no statistically significant between-group differences were observed with regard to age, parity, or postmenopausal status. Urethral length also did not differ significantly between the two groups.

Table 1. Sociodemographic and clinical characteristics of the study participants.

Variable	SUI ** (N = 20)		Continent controls (N = 20)		p-value
Age (years)	57.50 ± 12.60		54.15 ± 12.88		NS
Weight (kg)	82.95 ± 17.46		71.40 ± 16.72		0.03
BMI (kg/m ²)	30.30 ± 5.02		26.56 ± 6.16		0.02
Number of pregnancies	2.30 ± 1.08		2.05 ± 1.36		NS
Number of deliveries	2.05 ± 0.94		1.60 ± 0.88		NS
Urethral length (mm)	31.7 ± 6.0		30.0 ± 4.6		NS
Postmenopausal status, n (%)	5 (25%) (no)	15 (75%) (yes)	9 (45%) (no)	11 (55%) (yes)	NS

Continuous variables are presented as mean ± SD; categorical variables as n (%).

** Women with stress urinary incontinence

p-values were calculated using the χ^2 test for categorical variables and the independent-samples t-test or Wilcoxon rank-sum test for continuous variables, as appropriate.

Abbreviations: BMI = body mass index, N = number of participants, SD = standard deviation

Clinical findings suggestive of urethral dysfunction were more frequent in the SUI group. Urethral hypermobility during the Valsalva maneuver was observed in 12 participants (60.0%), and urethral funneling was detected in 8 participants (40.0%).

4.1.2. Strain elastography measurements

SE measurements at the EUO level in the control group deviated from a normal distribution, whereas SE values at all other ROIs met the assumption of normality. Detailed distributional characteristics are provided in the Supplementary Materials (**Table S1**).

MANOVA across the three anatomically defined urethral levels revealed a significant overall group effect (Wilks' $\lambda = 0.588$, $F(3,35) = 8.189$, $p < 0.001$), indicating statistically

significant differences in suburethral tissue elasticity between women with SUI and continent controls.

Across all urethral levels, women with SUI exhibited significantly higher strain values than continent controls (Games–Howell post hoc test, $p < 0.05$), consistent with reduced suburethral tissue stiffness. Mean strain values (\pm SD) in the SUI and control groups were 10.60 ± 8.19 versus 5.73 ± 3.45 at the IUO, 13.68 ± 7.24 versus 5.67 ± 3.21 at the MU, and 5.61 ± 4.95 versus 2.82 ± 2.26 at the EUO. These findings indicate increased tissue deformability across all suburethral regions in women with SUI. Greater inter-individual variability was observed in the SUI group (Figure 4).

A post hoc power analysis based on midurethral values yielded an observed Cohen’s d of 1.75, corresponding to a very large effect size. The analysis indicated that a minimum sample size of seven participants would have been sufficient to detect the observed effect.

Across the five repeated SE measurements obtained for each ROI, significant between-group differences were consistently observed, indicating increased tissue elasticity in the SUI cohort, with minor exceptions at the IUO level and in one of the five measurements at the EUO level (Table S2).

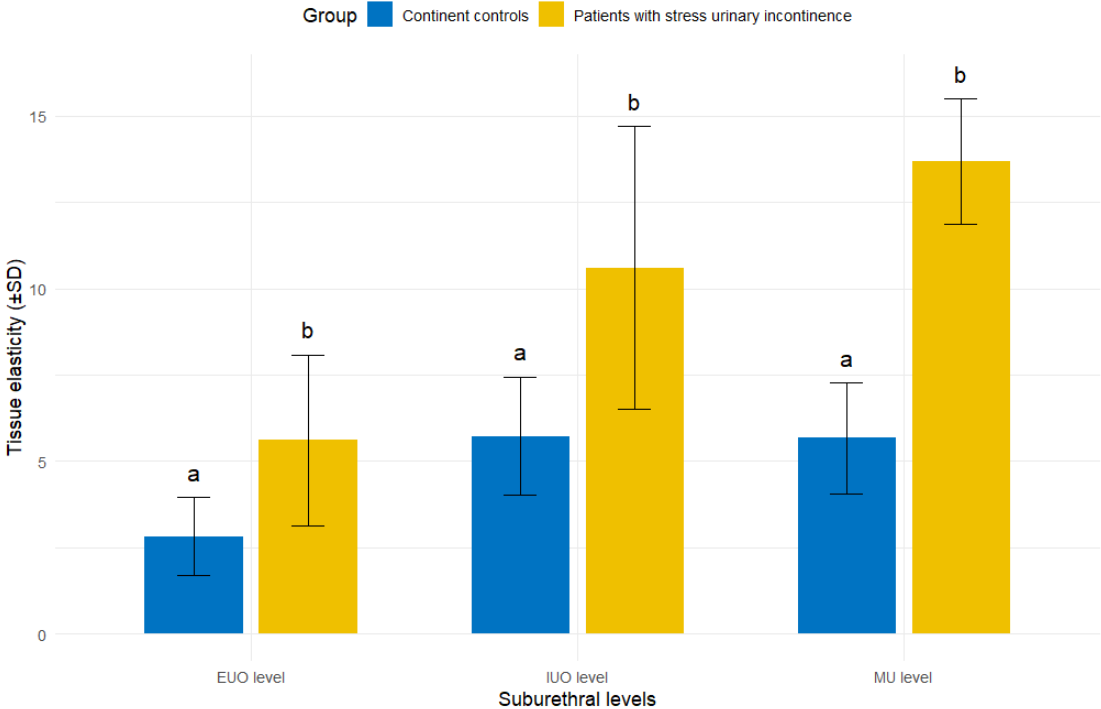


Figure 4. Comparison of suburethral tissue elasticity between continent women and women with stress urinary incontinence.

Bar plots show mean strain elastography values, reflecting relative tissue elasticity, at the external urethral orifice (EUO), internal urethral orifice (IUO), and midurethral (MU) levels. Error bars indicate standard deviations (SD). Different lowercase letters denote statistically significant between-group differences.

4.1.3. Reproducibility of strain elastography measurements

The reproducibility of repeated SE measurements was evaluated at three predefined anatomical levels: IUO, MU, and EUO, corresponding to the blue, purple, and green ROIs, respectively (**Figure 3**).

Internal consistency was assessed using Cronbach's alpha and demonstrated excellent reliability across all measurement sites in both the SUI and control groups. At the IUO level, Cronbach's alpha was 0.96 in both cohorts and remained essentially unchanged after data standardization (controls: 0.96; SUI: 0.97). Similarly high values were observed at the MU level (controls: 0.98; SUI: 0.95). The highest internal consistency was recorded at the EUO level (controls: 0.98; SUI: 0.99). Across all anatomical levels, Cronbach's alpha values exceeded 0.95, indicating excellent internal reliability.

These findings were corroborated by ICC analysis, confirming a high degree of measurement reproducibility. At the IUO level, ICC values were 0.969 (95% CI: 0.941–0.986) in controls and 0.962 (95% CI: 0.927–0.983) in the SUI group. At the MU level, ICCs reached 0.983 (95% CI: 0.968–0.993) in controls and 0.954 (95% CI: 0.913–0.980) in women with SUI. At the EUO level, ICC values were 0.978 (95% CI: 0.957–0.990) in controls and 0.991 (95% CI: 0.982–0.996) in the SUI group.

Taken together, these results demonstrate excellent measurement reliability and reproducibility across all suburethral ROIs in both study cohorts, supporting the methodological robustness of SE for assessing suburethral tissue stiffness (**Table 2**).

Table 2. Reproducibility of strain elastography measurements at each region of interest assessed by intraclass correlation coefficients (ICC)

Group	Internal urethral orifice (IUO)			Midurethral (MU)			External urethral orifice (EUO)		
	ICC	95% CI	<i>p</i> -value	ICC	95% CI	<i>p</i> -value	ICC	95% CI	<i>p</i> -value
Continent controls	0.96	0.94–0.98	<0.001	0.98	0.96–0.99	<0.001	0.97	0.95–0.99	<0.001
SUI **	0.96	0.92–0.98	<0.002	0.95	0.91–0.98	<0.002	0.99	0.98–0.99	<0.002

** Women with stress urinary incontinence

4.1.4. Diagnostic performance of strain elastography for stress urinary incontinence

ROC curve analysis was performed to evaluate the diagnostic performance of SE across the three predefined anatomical ROIs. Among these, the MU region demonstrated the highest discriminatory ability, with an AUC of 0.813 (95% CI: 0.666–0.960, $p < 0.001$). The EUO region showed moderate diagnostic performance (AUC = 0.763, 95% CI: 0.603–0.924, $p < 0.01$), whereas the IUO region yielded the lowest AUC value (0.728, 95% CI: 0.569–0.886, $p < 0.05$) (**Figure 5**).

ROC curves for SE measurements at the IUO, MU, and EUO regions are shown in **Figure 5**, with the dashed diagonal line indicating the reference line of no discrimination. Consistent with the AUC analysis, the MU region demonstrated the highest diagnostic accuracy, followed by the EUO and IUO regions.

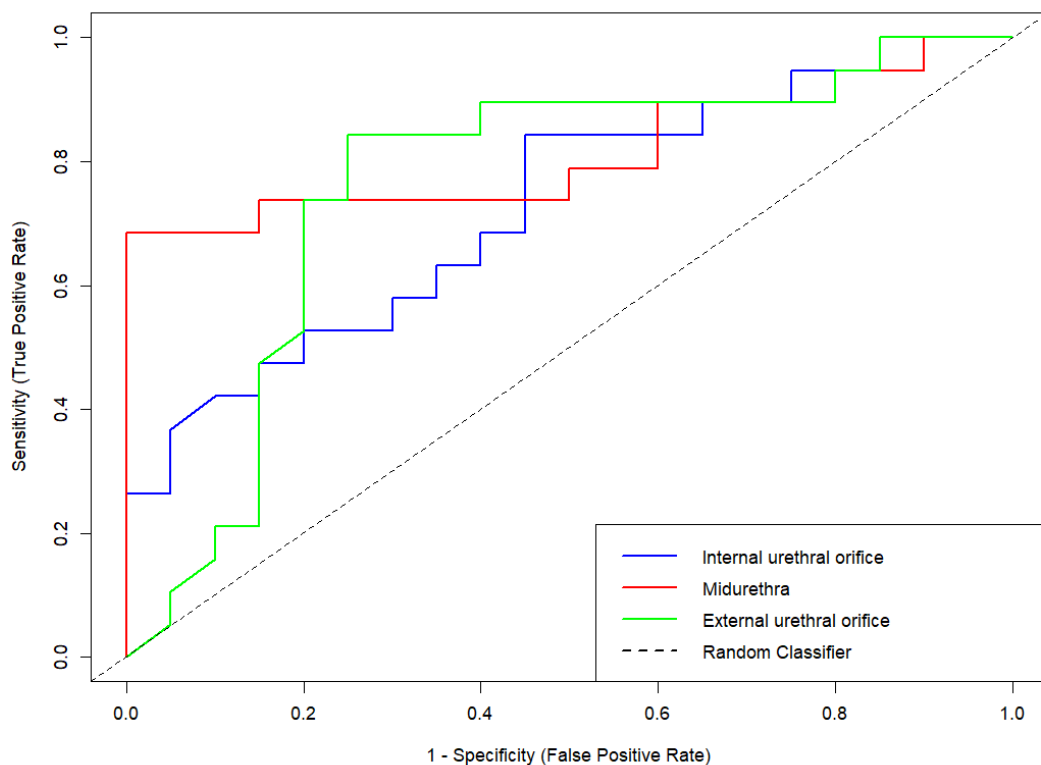


Figure 5. Receiver operating characteristic (ROC) curves for strain elastography across suburethral regions of interest in women with stress urinary incontinence.

A detailed summary of diagnostic performance metrics is provided in **Table 3**. Consistent with these findings, the MU region demonstrated the most favorable diagnostic profile (sensitivity: 0.65; specificity: 0.85). The EUO region demonstrated intermediate values (sensitivity: 0.60; specificity: 0.80), whereas the IUO region demonstrated the lowest values (sensitivity: 0.58; specificity: 0.70). Predictive values further supported the superior

performance of the MU region. Both the positive predictive value (PPV = 0.81) and negative predictive value (NPV = 0.71) were highest at the MU region. The EUO region showed moderately high predictive values (PPV = 0.75; NPV = 0.67), whereas the IUO region showed the lowest values (PPV = 0.65; NPV = 0.64). Balanced accuracy, calculated as the mean of sensitivity and specificity, was highest at the MU region (0.75), followed by the EUO (0.70) and IUO (0.64). This pattern paralleled the AUC values, further supporting the superior diagnostic performance of the MU region. Finally, the F1 score—the harmonic mean of precision and recall—was highest at the MU region (0.72), exceeding the values observed at the EUO (0.67) and IUO (0.61).

Overall, these findings indicate that the MU region represents the most diagnostically informative ROI for distinguishing women with SUI from continent controls.

Table 3. Diagnostic performance of strain elastography across anatomically defined regions of interest.

Categories	IUO	MU	EUO
Sensitivity or Recall $\frac{TP_i}{TP_i + FN_i}$	0.58	0.65	0.60
Specificity $\frac{TN_i}{TN_i + FP_i}$	0.70	0.85	0.80
Positive Predictive Value $PPV_i = \frac{TP_i}{TP_i + FP_i}$	0.65	0.81	0.75
Negative Predictive Value $NPV_i = \frac{TN_i}{TN_i + FN_i}$	0.64	0.71	0.67
Prevalence $\frac{TP_i + FN_i}{N}$	0.49	0.50	0.50
Detection Rate $\frac{TP_i}{N}$	0.28	0.33	0.30
Detection Prevalence $\frac{TP_i + FP_i}{N}$	0.44	0.40	0.40
Balanced Accuracy $\frac{Sensitivity_i + Specificity_i}{2}$	0.64	0.75	0.70
Area Under the ROC Curve	0.72	0.81	0.76
F1 score $\frac{2 \cdot PPV \cdot Sensitivity}{PPV + Sensitivity}$	0.61	0.72	0.67

Abbreviations: EUO = external urethral orifice, FN = false negative, FP = false positive, IUO = internal urethral orifice, MU = midurethra, N = number of participants, NPV = negative predictive value, PPV = positive predictive value, ROC = receiver operating characteristic, TN = true negative, TP = true positive

4.2. Results of the structured literature review

The structured PubMed search identified 19 records. After removal of three duplicates, 16 articles remained for title and abstract screening. Following full-text assessment based on the predefined eligibility criteria, 12 studies were included in the qualitative synthesis (**Table 4**). The study selection process is illustrated in **Figure 6**.

Table 4. Summary of elastography studies included in the literature analysis.

References	Author, Year	Modality
[24]	Kreutzkamp et al., 2017	SE
[42]	Yu et al., 2021	SE
[43]	Csákány et al., 2025	SE
[16]	Petros, 2003	Biomechanical concepts
[20]	Jamard et al., 2020	Review
[44]	Zhao et al., 2020	SWE
[45]	Okcu et al., 2021	SWE
[25]	Ptaszkowski et al., 2021	SWE
[46]	Li et al., 2022	SWE
[47]	Wang et al., 2023	SWE
[30]	Li et al., 2024	SWE
[14]	De Vicari et al., 2025	SWE

Abbreviations: SE = strain elastography, SWE = shear wave elastography

Only a limited number of studies have specifically evaluated SE of suburethral tissues in women with SUI, indicating that direct assessment of suburethral biomechanical properties remains underrepresented in the current literature. Across the available studies, women with SUI consistently demonstrate altered periurethral or pelvic floor biomechanical characteristics compared with continent controls, including reduced tissue stiffness, increased deformability, and impaired load-dependent urethral support.

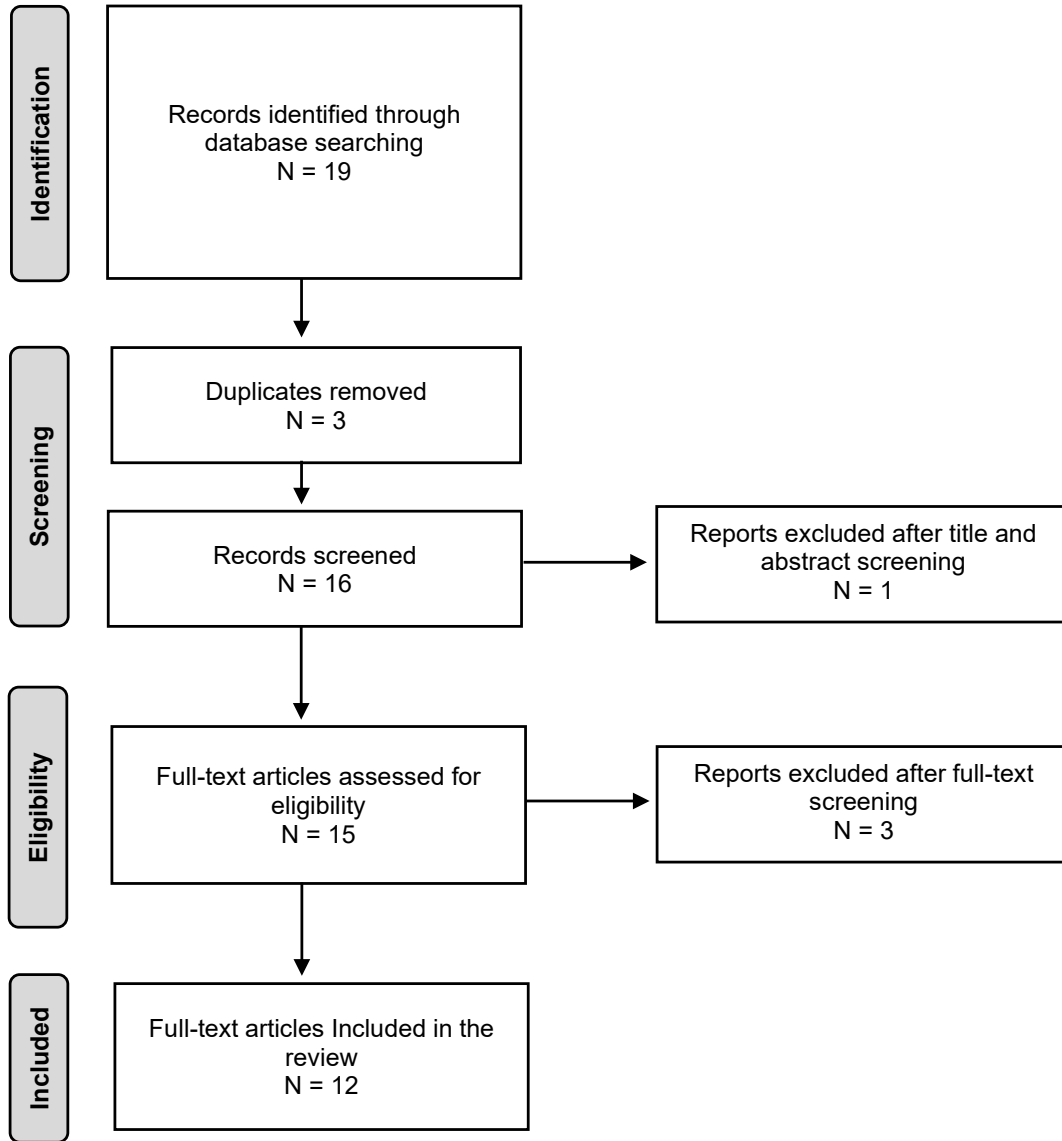


Figure 6. Flow diagram illustrating the study selection process for the literature review.
Abbreviations: N = number of records

5. DISCUSSION

SUI is a highly prevalent pelvic floor disorder characterized by impaired suburethral support and associated with considerable physical, psychosocial, and socioeconomic burden [1, 14, 28, 30]. Although perineal and introital ultrasound are widely used in urogynecological imaging, their diagnostic value is largely limited to the assessment of anatomical configuration and kinematic displacement, providing only indirect information about the mechanical competence of tissues responsible for continence [6, 9, 19, 28, 30]. This limitation underscores the need for functional imaging techniques capable of characterizing pelvic floor biomechanics *in vivo*.

Elastography represents a methodological extension of conventional ultrasound by enabling the assessment of tissue deformation behavior and stiffness—parameters directly involved in continence mechanisms [21, 24, 46].

The present thesis demonstrates that standardized introital SE is a feasible, reproducible, and clinically informative imaging modality for the functional assessment of suburethral tissue biomechanics in women with clinically confirmed pure SUI.

Furthermore, the structured literature analysis indicates that only a limited number of studies have investigated the relationship between SE-derived biomechanical parameters and SUI in women. Consequently, the application of SE for direct evaluation of suburethral support mechanisms remains relatively underexplored, highlighting the scientific novelty and clinical relevance of the present work within urogynecological imaging.

5.1. Interpretation of the main findings

The principal finding of this work is that women with SUI exhibit significantly higher SE values across all anatomically predefined suburethral ROIs, indicating reduced tissue stiffness and increased deformability compared with continent controls. These differences were consistently observed at the IUO, MU, and EUO levels, with the most pronounced discriminatory performance at the MU level.

From a biomechanical perspective, increased tissue deformability reflects diminished load-bearing capacity and reduced resistance to stress-related deformation. This observation is consistent with contemporary biomechanical models of continence, which emphasize that effective urethral closure during increases in intra-abdominal pressure depends primarily on the stiffness and coordinated mechanical behavior of the suburethral support system rather than on urethral position alone [2, 5–7]. Excessive deformation of this support layer compromises pressure transmission, resulting in urethral hypermobility and stress-induced urinary leakage [2, 5, 6].

The superior diagnostic performance observed at the midurethral level is particularly noteworthy, as this region represents the biomechanical core of urethral support, where the endopelvic fascia, anterior vaginal wall, and levator ani muscle interact. The present findings provide direct in vivo functional evidence supporting the central role of midurethral support failure in SUI, in accordance with the hammock hypothesis [5, 6].

5.2. Comparison with previous strain elastography studies

To date, only limited data are available regarding the application of SE for the evaluation of suburethral biomechanics. The feasibility study by Kreutzkamp et al. did not demonstrate a significant association between periurethral elasticity and urinary incontinence. However, several methodological differences likely explain the discrepancy with the present findings. These include heterogeneous incontinence phenotypes, the absence of anatomically standardized ROI placement, lack of internal reference normalization, and the omission of reproducibility analyses [24].

In contrast, the present thesis applied anatomically predefined ROIs at three distinct urethral levels and normalized strain values to periurethral adipose tissue, thereby reducing variability related to probe pressure, tissue depth, and imaging geometry. These methodological refinements enabled the detection of consistent, level-specific biomechanical differences that were not captured in earlier exploratory studies.

5.3. Reproducibility and methodological robustness

A major methodological strength of this study is the excellent reproducibility of SE measurements across all examined suburethral regions. Both ICC and Cronbach's alpha values exceeded thresholds for excellent reliability in the SUI and control groups, demonstrating high internal consistency of repeated measurements.

These findings address a common concern associated with SE, namely its potential operator dependence. The present results indicate that rigorous protocol standardization—including anatomically anchored ROI placement and internal reference-tissue normalization—substantially reduces this limitation. Consequently, introital SE can provide reliable biomechanical information when applied within a standardized methodological framework.

5.4. Obstetric contributions to suburethral biomechanical impairment

Biomechanical impairment of the suburethral support system in SUI is partly attributable to childbirth-related mechanical trauma. Vaginal delivery is associated with a substantially higher risk of SUI than cesarean section, a difference largely explained by injury to urethral support structures and sphincteric function. The occurrence of de novo SUI in previously continent women after childbirth—characterized by reduced maximal urethral closure pressure and increased bladder neck mobility—further suggests that continence failure reflects underlying biomechanical vulnerability rather than parity alone [9, 30].

During a prolonged second stage of labor, the levator ani muscle and associated perineal structures may undergo extreme elongation, exceeding three times their resting length. Under these conditions, eccentric contraction of the pubovisceral muscle fibers can generate tensile forces beyond their ultimate tensile capacity, resulting in partial or complete avulsion from the pubic bone. This mechanism is widely recognized as the principal cause of levator ani avulsion and represents a critical injury to the pelvic floor support apparatus [9, 13].

Structural correlates of these injuries have been demonstrated by MRI, including enlargement of the levator hiatus, rotation of the perineal membrane, and lateral detachment of the levator ani muscle—phenomena collectively described as the “swinging-door” mechanism. These alterations lead to persistent mechanical instability, reduced suburethral stiffness, and impaired pressure transmission within the pelvic floor, thereby providing a biomechanical explanation for postpartum SUI [8, 9].

Consistent with these biomechanical and structural observations, epidemiological studies indicate that vaginal delivery is associated with an approximately 67% increase in long-term SUI risk compared with cesarean section, with operative vaginal delivery conferring an even greater risk [14, 48].

5.5. Relationship of the present findings to previous elastography and biomechanical research

Evidence from SWE studies supports the biomechanical interpretation of the present findings. Reduced stiffness of key pelvic floor structures—particularly the levator ani muscle and the perineal body—has been consistently reported in women with SUI, reflecting impaired load-dependent stiffening [30, 46]. These observations are consistent with the SE findings of the present study, demonstrating increased suburethral deformability and reduced stiffness within the urethral support system.

Although SE and SWE rely on different technical principles, they provide complementary biomechanical information. SE evaluates relative tissue deformation during routine introital imaging, whereas SWE provides operator-independent quantitative measurements of tissue stiffness. Despite these methodological differences, both techniques support a common conceptual model of SUI as a disorder of impaired force transmission and deficient load transfer within the pelvic floor, rather than a condition defined solely by anatomical displacement [14, 21, 49].

Interventional elastography studies further reinforce this interpretation. Yu et al. demonstrated reduced levator ani stiffness in women with SUI both at rest and during the Valsalva maneuver, with stiffness increasing in parallel with clinical improvement following pelvic floor muscle training [42]. Similarly, Li et al. reported diminished load-dependent stiffening of the perineal body, with SWE measurements obtained during Valsalva demonstrating high specificity for predicting SUI [30]. Together, these findings indicate that impaired mechanical responsiveness to stress represents a key functional characteristic of SUI.

An apparent exception was reported by De Vicari et al., who observed increased midurethral stiffness in women with SUI using SWE [14]. This discrepancy may reflect compensatory fibrosis or maladaptive remodeling of the urethral wall secondary to chronically insufficient supportive tension. Importantly, whereas most elastographic studies—including the present investigation—focus on the fibromuscular suburethral support layer, De Vicari et al. evaluated the urethral wall itself. This distinction supports the concept of dual-level dysfunction in SUI, involving both weakened suburethral load transfer and region-specific alterations of the urethral wall or sphincteric complex [14, 30]. Complementary evidence from supersonic shear imaging further indicates reduced rhabdosphincter stiffness correlating with symptom severity, suggesting intrinsic sphincteric softening as an additional contributory mechanism [44].

Biomechanical modeling studies provide additional support for this integrated interpretation. Virtual operation experiments by Petros and colleagues demonstrated that restoration of tension within the suburethral support layer leads to immediate improvement in urethral pressure transmission, illustrating a tension-dependent musculoelastic continence mechanism [16]. This model closely aligns with elastographic observations of reduced suburethral stiffness and impaired force transmission in women with SUI [5, 11].

Finally, multimodal ultrasound studies provide further corroboration. Wang et al. reported increased bladder neck mobility, greater urethral rotation, and reduced urethral sphincter elasticity in women with SUI, findings consistent with compromised urethral closure mechanics [47].

5.6. Limitations and future perspectives

Several limitations of this study should be acknowledged. First, the investigation was conducted at a single center with a relatively limited sample size, which may restrict the generalizability of the findings. Although excellent intra-observer reproducibility was demonstrated, inter-observer reliability, multicenter validation, and cross-platform calibration were not evaluated.

In addition, SE remains a qualitative and semi-quantitative technique and may be influenced by factors such as probe precompression, transducer orientation, and tissue heterogeneity, despite the use of standardized acquisition protocols.

Emerging technological developments—including automated ROI detection, three-dimensional elastography, and artificial intelligence–based analytical approaches—may further improve measurement reproducibility, reduce operator dependence, and facilitate broader clinical implementation of elastographic techniques [50–52].

5.7. Clinical implications

Standardized introital SE provides biomechanical information that complements conventional pelvic floor ultrasound imaging [21, 47]. SE-derived stiffness patterns may support treatment planning by helping identify patients in whom impaired midurethral support represents a dominant biomechanical contributor to SUI.

The demonstrated feasibility and reproducibility of the technique also suggest potential utility for longitudinal monitoring of therapeutic interventions—including pelvic floor muscle training, conservative management, and surgical treatment—by enabling objective assessment of tissue-level mechanical changes over time.

Although diagnostic cut-off values cannot yet be established, the present findings provide a strong rationale for validation in larger multicenter cohorts. By enabling *in vivo* assessment of pelvic floor biomechanics, standardized introital SE may facilitate a transition in pelvic floor imaging from predominantly morphological evaluation toward functional tissue characterization.

6. CONCLUSION

SUI is increasingly conceptualized as a disorder of pelvic floor biomechanics in which continence failure reflects impaired mechanical integrity of the suburethral support system. Despite this evolving pathophysiological understanding, routine imaging remains largely limited to anatomical and kinematic assessment and does not directly evaluate tissue-level mechanical competence.

This thesis demonstrates that standardized introital SE represents a feasible, reproducible, and clinically informative modality for the *in vivo* functional assessment of suburethral tissue biomechanics in women with clinically confirmed pure SUI. The use of anatomically predefined ROIs combined with internal reference-tissue normalization enabled reliable qualitative and semi-quantitative characterization of periurethral stiffness. The literature analysis further indicates that elastographic evaluation of suburethral support has not yet been systematically incorporated into SUI diagnostics. The present study therefore contributes to addressing this gap by providing structured *in vivo* biomechanical data.

Women with SUI exhibited consistently increased tissue deformability across all examined suburethral levels compared with continent controls, reflecting reduced mechanical stiffness of the urethral support system. The midurethral region demonstrated the strongest discriminatory performance, identifying it as the most biomechanically informative site of continence failure. These findings provide *in vivo* functional evidence supporting contemporary biomechanical models that attribute SUI to impaired load transfer within the suburethral support platform.

High measurement reproducibility and internal consistency confirm that SE provides reliable biomechanical information when applied under standardized conditions. Together with converging evidence from SWE and biomechanical modeling studies, these results support a unified mechanistic interpretation of SUI as a disorder of impaired force transmission and deficient load-dependent stiffening within pelvic floor support structures.

In conclusion, standardized introital SE represents a methodologically robust tool for the functional characterization of suburethral mechanical integrity. The present work provides a foundation for future validation studies aimed at defining clinically meaningful thresholds and integrating biomechanical imaging into mechanism-based phenotyping, treatment stratification, and longitudinal outcome assessment in women with SUI.

ACKNOWLEDGEMENTS

I would like to express my sincere gratitude to all those who contributed to the completion of this thesis.

I am deeply indebted to Prof. Gábor Németh and Prof. Szabolcs Várbíró, the former and current heads of the department, for providing the institutional support that enabled my research at the Department of Obstetrics and Gynecology, Albert Szent-Györgyi Medical School, University of Szeged.

I am particularly grateful to my supervisors, Dr. Norbert Pásztor and Prof. Gábor Németh, for their continuous guidance, scientific insight, and constructive criticism throughout the planning, execution, and completion of this research.

My sincere thanks also go to Dr. Andrea Surányi for her valuable contribution to the acquisition of the strain elastography images.

I am grateful to Flórián Kovács for his valuable assistance with the statistical analyses.

I also thank Marianna Szabó for her professional collaboration, support in patient recruitment, and assistance during data acquisition.

Above all, I would like to express my deepest gratitude to my family. I am profoundly thankful to my wife, Noémi, for her unwavering support, patience, and understanding throughout the demanding period of this work, and to my daughter, Hanna, for her patience and acceptance during the many hours devoted to research and writing.

Finally, I extend my heartfelt thanks to the participating patients, whose willingness and cooperation made this research possible.

REFERENCES

1. Haylen BT, De Ridder D, Freeman RM, et al (2010) An International Urogynecological Association (IUGA)/International Continence Society (ICS) joint report on the terminology for female pelvic floor dysfunction. *Int Urogynecol J* 21:5–26. <https://doi.org/10.1007/s00192-009-0976-9>
2. Lugo T, Leslie SW, Mikes BA, Riggs J (2025) Stress Urinary Incontinence. In: StatPearls. StatPearls Publishing, Treasure Island (FL)
3. Chong EC, Khan AA, Anger JT (2011) The financial burden of stress urinary incontinence among women in the United States. *Curr Urol Rep* 12:358–362. <https://doi.org/10.1007/s11934-011-0209-x>
4. Chen Y, DeSautel M, Anderson A, et al (2004) Collagen synthesis is not altered in women with stress urinary incontinence. *Neurourology and Urodynamics* 23:367–373. <https://doi.org/10.1002/nau.20006>
5. DeLancey JO (1994) Structural support of the urethra as it relates to stress urinary incontinence: the hammock hypothesis. *Am J Obstet Gynecol* 170:1713–1720; discussion 1720-1723. [https://doi.org/10.1016/s0002-9378\(94\)70346-9](https://doi.org/10.1016/s0002-9378(94)70346-9)
6. Ashton-Miller JA, DeLANCEY JOL (2007) Functional Anatomy of the Female Pelvic Floor. *Annals of the New York Academy of Sciences* 1101:266–296. <https://doi.org/10.1196/annals.1389.034>
7. Falconer C, Ekman-Ordeberg G, Blomgren B, et al (1998) Paraurethral connective tissue in stress-incontinent women after menopause. *Acta Obstet Gynecol Scand* 77:95–100. <https://doi.org/10.1080/00016349808565820>
8. Pipitone F, Swenson CW, DeLancey JOL, Chen L (2021) Novel 3D MRI technique to measure perineal membrane structural changes with pregnancy and childbirth: Technique development and measurement feasibility. *Int Urogynecol J* 32:2413–2420. <https://doi.org/10.1007/s00192-021-04795-x>
9. DeLancey JOL, Masteling M, Pipitone F, et al (2024) Pelvic floor injury during vaginal birth is life-altering and preventable: what can we do about it? *American Journal of Obstetrics and Gynecology* 230:279-294.e2. <https://doi.org/10.1016/j.ajog.2023.11.1253>
10. Song Y, Hong X, Yu Y, Lin Y (2007) Changes of collagen type III and decorin in paraurethral connective tissue from women with stress urinary incontinence and prolapse. *Int Urogynecol J* 18:1459–1463. <https://doi.org/10.1007/s00192-007-0356-2>
11. Falconer C, Ekman-Ordeberg G, Ulmsten U, et al (1996) Changes in paraurethral connective tissue at menopause are counteracted by estrogen. *Maturitas* 24:197–204. [https://doi.org/10.1016/s0378-5122\(96\)82010-x](https://doi.org/10.1016/s0378-5122(96)82010-x)
12. Chen Y, Peng L, Liu M, et al (2023) Diagnostic value of transperineal ultrasound in patients with stress urinary incontinence (SUI): a systematic review and meta-analysis. *World J Urol* 41:687–693. <https://doi.org/10.1007/s00345-022-04264-0>

13. Dietz HP, Lanzarone V (2005) Levator Trauma After Vaginal Delivery: *Obstetrics & Gynecology* 106:707–712. <https://doi.org/10.1097/01.AOG.0000178779.62181.01>
14. De Vicari D, Barba M, Costa C, et al (2025) Assessment of Urethral Elasticity by Shear Wave Elastography: A Novel Parameter Bridging a Gap Between Hypermobility and ISD in Female Stress Urinary Incontinence. *Bioengineering* 12:373. <https://doi.org/10.3390/bioengineering12040373>
15. Kozma B, Pákozdy K, Lampé R, et al (2021) Ultrahang-elasztográfia alkalmazásának lehetőségei a szülészet-nőgyógyászatban. <https://doi.org/10.1556/650.2021.32094>
16. Petros P (2003) Changes in bladder neck geometry and closure pressure after midurethral anchoring suggest a musculoelastic mechanism activates closure. *Neurourology and Urodynamics* 22:191–197. <https://doi.org/10.1002/nau.10085>
17. Dietz HP (2010) Pelvic floor ultrasound: a review. *Am J Obstet Gynecol* 202:321–334. <https://doi.org/10.1016/j.ajog.2009.08.018>
18. Zhong C, Hu P, Ran S, et al (2023) Association Between Urinary Stress Incontinence and Levator Avulsion Detected by 3D Transperineal Ultrasound. *Ultraschall Med* 44:e39–e46. <https://doi.org/10.1055/a-1497-1838>
19. Gupta AP, Pandya PR, Nguyen M-L, et al (2018) Use of Dynamic MRI of the Pelvic Floor in the Assessment of Anterior Compartment Disorders. *Curr Urol Rep* 19:112. <https://doi.org/10.1007/s11934-018-0862-4>
20. Jamard E, Blouet M, Thubert T, et al (2020) Utility of 2D-ultrasound in pelvic floor muscle contraction and bladder neck mobility assessment in women with urinary incontinence. *Journal of Gynecology Obstetrics and Human Reproduction* 49:101629. <https://doi.org/10.1016/j.jogoh.2019.101629>
21. Dietrich C, Barr R, Farrokh A, et al (2017) Strain Elastography - How To Do It? *Ultrasound Int Open* 03:E137–E149. <https://doi.org/10.1055/s-0043-119412>
22. Bamber J, Cosgrove D, Dietrich C, et al (2013) EFSUMB Guidelines and Recommendations on the Clinical Use of Ultrasound Elastography. Part 1: Basic Principles and Technology. *Ultraschall in Med* 34:169–184. <https://doi.org/10.1055/s-0033-1335205>
23. Gennisson J-L, Deffieux T, Fink M, Tanter M (2013) Ultrasound elastography: Principles and techniques. *Diagnostic and Interventional Imaging* 94:487–495. <https://doi.org/10.1016/j.diii.2013.01.022>
24. Kreutzkamp JM, Schäfer SD, Amler S, et al (2017) Strain Elastography as a New Method for Assessing Pelvic Floor Biomechanics. *Ultrasound in Medicine & Biology* 43:868–872. <https://doi.org/10.1016/j.ultrasmedbio.2016.12.004>
25. Ptaszkowski K, Małkiewicz B, Zdrojowy R, et al (2021) Assessment of the Elastographic and Electromyographic of Pelvic Floor Muscles in Postmenopausal Women with Stress Urinary Incontinence Symptoms. *Diagnostics* 11:2051. <https://doi.org/10.3390/diagnostics11112051>

26. Kang H (2021) Sample size determination and power analysis using the G*Power software. *J Educ Eval Health Prof* 18:17. <https://doi.org/10.3352/jeehp.2021.18.17>
27. Tunn R, Petri E (2003) Introital and transvaginal ultrasound as the main tool in the assessment of urogenital and pelvic floor dysfunction: an imaging panel and practical approach. *Ultrasound in Obstet & Gyne* 22:205–213. <https://doi.org/10.1002/uog.189>
28. Nambiar AK, Arlandis S, Bø K, et al (2022) European Association of Urology Guidelines on the Diagnosis and Management of Female Non-neurogenic Lower Urinary Tract Symptoms. Part 1: Diagnostics, Overactive Bladder, Stress Urinary Incontinence, and Mixed Urinary Incontinence. *European Urology* 82:49–59. <https://doi.org/10.1016/j.eururo.2022.01.045>
29. Oliveira FR, Ramos JGL, Martins-Costa S (2006) Translabial Ultrasonography in the Assessment of Urethral Diameter and Intrinsic Urethral Sphincter Deficiency. *Journal of Ultrasound in Medicine* 25:1153–1158. <https://doi.org/10.7863/jum.2006.25.9.1153>
30. Li X, Zhang L, Li Y, et al (2024) Assessment of perineal body properties in women with stress urinary incontinence using Transperineal shear wave elastography. *Sci Rep* 14:21647. <https://doi.org/10.1038/s41598-024-72429-5>
31. Ophir J, Céspedes I, Ponnekanti H, et al (1991) Elastography: a quantitative method for imaging the elasticity of biological tissues. *Ultrason Imaging* 13:111–134. <https://doi.org/10.1177/016173469101300201>
32. Ciraci S, Tan S, Ozcan AS, et al (2015) Contribution of real-time elastography in diagnosis of polycystic ovary syndrome. *Diagn Interv Radiol* 21:118–122. <https://doi.org/10.5152/dir.2014.14094>
33. Mazloomdoost D, Westermann LB, Mutema G, et al (2017) Histologic Anatomy of the Anterior Vagina and Urethra. *Female Pelvic Med Reconstr Surg* 23:329–335. <https://doi.org/10.1097/SPV.0000000000000387>
34. De Landsheere L, Munaut C, Nusgens B, et al (2013) Histology of the vaginal wall in women with pelvic organ prolapse: a literature review. *Int Urogynecol J* 24:2011–2020. <https://doi.org/10.1007/s00192-013-2111-1>
35. Jung J, Ahn HK, Huh Y (2012) Clinical and Functional Anatomy of the Urethral Sphincter. *Int Neurourol J* 16:102. <https://doi.org/10.5213/inj.2012.16.3.102>
36. Pomian A, Majkusiak W, Kociszewski J, et al (2018) Demographic features of female urethra length. *Neurourology and Urodynamics* 37:1751–1756. <https://doi.org/10.1002/nau.23509>
37. Tierney L (2012) The R Statistical Computing Environment. In: Feigelson ED, Babu GJ (eds) *Statistical Challenges in Modern Astronomy V*. Springer New York, New York, NY, pp 435–447
38. Zhang L, Dong Y-J, Zhou J-Q, et al (2020) Similar Reproducibility for Strain and Shear Wave Elastography in Breast Mass Evaluation: A Prospective Study Using the Same Ultrasound System. *Ultrasound in Medicine & Biology* 46:981–991. <https://doi.org/10.1016/j.ultrasmedbio.2019.12.017>

39. Koo TK, Li MY (2016) A Guideline of Selecting and Reporting Intraclass Correlation Coefficients for Reliability Research. *Journal of Chiropractic Medicine* 15:155–163. <https://doi.org/10.1016/j.jcm.2016.02.012>
40. Mandrekar JN (2010) Receiver Operating Characteristic Curve in Diagnostic Test Assessment. *Journal of Thoracic Oncology* 5:1315–1316. <https://doi.org/10.1097/JTO.0b013e3181ec173d>
41. Madarász B, Jakab G, Szalai Z, et al (2021) Long-term effects of conservation tillage on soil erosion in Central Europe: A random forest-based approach. *Soil and Tillage Research* 209:104959. <https://doi.org/10.1016/j.still.2021.104959>
42. Yu H, Zheng H, Zhang X, et al (2021) Association between elastography findings of the levator ani and stress urinary incontinence. *Journal of Gynecology Obstetrics and Human Reproduction* 50:101906. <https://doi.org/10.1016/j.jogoh.2020.101906>
43. Csákány L, Kozinszky Z, Kovács F, et al (2025) Evaluation of Suburethral Tissue Elasticity Using Strain Elastography in Women with Stress Urinary Incontinence. *JCM* 14:5617. <https://doi.org/10.3390/jcm14165617>
44. Zhao B, Wen L, Chen W, et al (2020) A Preliminary Study on Quantitative Quality Measurements of the Urethral Rhabdosphincter Muscle by Supersonic Shear Wave Imaging in Women With Stress Urinary Incontinence. *J of Ultrasound Medicine* 39:1615–1621. <https://doi.org/10.1002/jum.15255>
45. Okcu NT, Vuruskan E, Gorgulu FF (2021) Use of Shear Wave Elastography to Evaluate Stress Urinary Incontinence in Women. *J Coll Physicians Surg Pak* 31:1196–1201. <https://doi.org/10.29271/jcpsp.2021.10.1196>
46. Li XM, Zhang LM, Li Y, et al (2022) Usefulness of transperineal shear wave elastography of levator ani muscle in women with stress urinary incontinence. *Abdom Radiol* 47:1873–1880. <https://doi.org/10.1007/s00261-022-03478-5>
47. Wang L, Liu Y, Wang X, et al (2023) Association between urethral funneling in stress urinary incontinence and the biological properties of the urethral rhabdosphincter muscle based on shear wave elastography. *Neurourology and Urodynamics* 42:282–288. <https://doi.org/10.1002/nau.25080>
48. Rortveit G, Daltveit AK, Hannestad YS, et al (2003) Urinary incontinence after vaginal delivery or cesarean section. *N Engl J Med* 348:900–907. <https://doi.org/10.1056/NEJMoa021788>
49. Yang J-M, Huang W-C (2023) Ultrasound in Female Urinary Incontinence. *J Med Ultrasound* 32:14–20. https://doi.org/10.4103/jmu.jmu_25_23
50. Szabó G, Madár I, et al (2022) A novel complementary method for ultrasonographic screening of deep endometriosis: a case series of 5 patients diagnosed with transvaginal strain elastography. *Clin Exp Obstet Gynecol* 49:1. <https://doi.org/10.31083/j.ceog4901002>

51. Huang X, Wang D, Li S, et al (2024) Advancements in artificial intelligence for pelvic floor ultrasound analysis. *Am J Transl Res* 16:1037–1043. <https://doi.org/10.62347/JXQQ5395>
52. Zhang M, Lin X, Zheng Z, et al (2022) Artificial intelligence models derived from 2D transperineal ultrasound images in the clinical diagnosis of stress urinary incontinence. *Int Urogynecol J* 33:1179–1185. <https://doi.org/10.1007/s00192-021-04859-y>

SUPPLEMENTARY MATERIALS

Normality of the SE data was assessed using the Kolmogorov–Smirnov test. At the IUO level, SE values were normally distributed in both the control and SUI groups (both $p > 0.05$). A normal distribution was also observed at the MU level in both cohorts ($p > 0.05$). In contrast, measurements at the EUO level deviated significantly from normality in the control group ($p < 0.05$), whereas the SUI group satisfied the normality assumption ($p > 0.05$).

These findings were further supported by descriptive distribution metrics. At the IUO level, the SUI group exhibited higher skewness and kurtosis (skewness: 2.24; kurtosis: 6.80) compared with controls (skewness: 0.88; kurtosis: 0.52). At the MU level, both groups demonstrated distributions approximating normality, with only minor skewness and kurtosis (controls: skewness 0.44, kurtosis -0.44 ; SUI: skewness -0.18 , kurtosis -0.66). At the EUO level, elevated skewness (1.65) and kurtosis (1.95) were observed in the control group, whereas values in the SUI group were closer to those expected under a normal distribution (skewness: 0.41; kurtosis: -0.11). Overall, the assumption of normality was satisfied for all datasets except EUO measurements in the control group (**Table S1**).

Measurement reproducibility was evaluated using ICCs calculated across five repeated SE acquisitions per ROI. In most cases, ICC values exceeded 0.80, indicating good to excellent repeatability (**Figures S1–S3**). Although repeated-measures ANOVA revealed significant within-group variation at the IUO level in controls ($p = 0.031$) and at the MU level in the SUI group ($p = 0.003$), ICC values remained consistently high (IUO: 0.78–0.91; MU: 0.71–0.92). This pattern suggests that the observed variability primarily reflects physiological heterogeneity rather than measurement inconsistency (**Table S1**).

Table S1. Distribution and normality of strain elastography values across urethral regions of interest in women with stress urinary incontinence versus continent controls.

Anatomical ROIs		Kolmogorov–Smirnov test			Descriptives		
		Statistic	<i>p</i> -value	result	Skewness	Kurtosis	median
IUO	Controls	0.182	0.098	TRUE	0.882	0.528	4.5780
	SUI**	0.171	0.175	TRUE	2.240	6.808	9.1020
MU	Controls	0.092	0.2	TRUE	0.437	-0.442	5.2800
	SUI**	0.182	0.118	TRUE	-0.177	-0.659	15.1000
EUO	Controls	0.245	0.004	FALSE	1.647	1.948	1.7040
	SUI**	0.105	0.2	TRUE	0.408	-0.112	4.2000

** Women with stress urinary incontinence

Abbreviations: EUO = external urethral orifice, IUO = internal urethral orifice, MU = midurethra

Table S2. Strain elastography measurements across anatomically defined regions of interest in study participants*

	Continent controls (Mean ± SD)	SUI** (Mean ± SD)	<i>p</i> -value	95% CI
SE measurements at the level of IUO ^{††}				
Measurement 1	6.52 ± 4.21	10.98 ± 9.14	0.06	−9.08 – −0.16
Measurement 2	5.64 ± 3.99	10.19 ± 8.12	0.03	−8.65 – −0.45
Measurement 3	5.3 ± 3.27	10.93 ± 8.88	0.01	−9.99 – −1.26
Measurement 4	5.31 ± 3.17	9.01 ± 7.88	0.06	−7.55 – 0.15
Measurement 5	6.14 ± 3.46	9.98 ± 9.08	0.09	−8.33 – 0.64
SE measurements at the level of MU ^{††}				
Measurement 1	5.92 ± 3.50	14.29 ± 8.68	<0.001	−12.68 – −4.06
Measurement 2	5.60 ± 3.23	12.67 ± 7.21	<0.001	−10.70 – −3.44
Measurement 3	5.45 ± 3.37	13.38 ± 7.59	<0.001	−11.75 – −4.12
Measurement 4	5.35 ± 3.06	12.59 ± 7.74	0.001	−11.08 – −3.41
Measurement 5	6.01 ± 3.38	13.53 ± 8.18	0.001	−11.59 – −3.45
SE measurements at the level of EUO ^{††}				
Measurement 1	3.28 ± 2.74	5.39 ± 4.12	0.06	−4.34 – 0.13
Measurement 2	2.95 ± 2.20	5.58 ± 5.42	0.05	−5.28 – 0.02
Measurement 3	2.76 ± 2.34	5.47 ± 4.82	0.03	−5.13 – −0.28
Measurement 4	2.39 ± 2.11	5.29 ± 5.61	0.04	−5.61 – −0.19
Measurement 5	2.73 ± 2.27	5.51 ± 4.74	0.02	−5.16 – −0.40

* All continuous variables are expressed as mean ± standard deviation.

** Women with stress urinary incontinence

†† Measurements were performed at three anatomical ROIs, visualized on elastographic images as color-coded regions: blue = IUO, purple = MU, green = EUO (Figure 3).

p-values were calculated using the unpaired t-test or Wilcoxon rank-sum test, as appropriate.

Abbreviations: EUO = external urethral orifice, IUO = internal urethral orifice, MU = midurethra

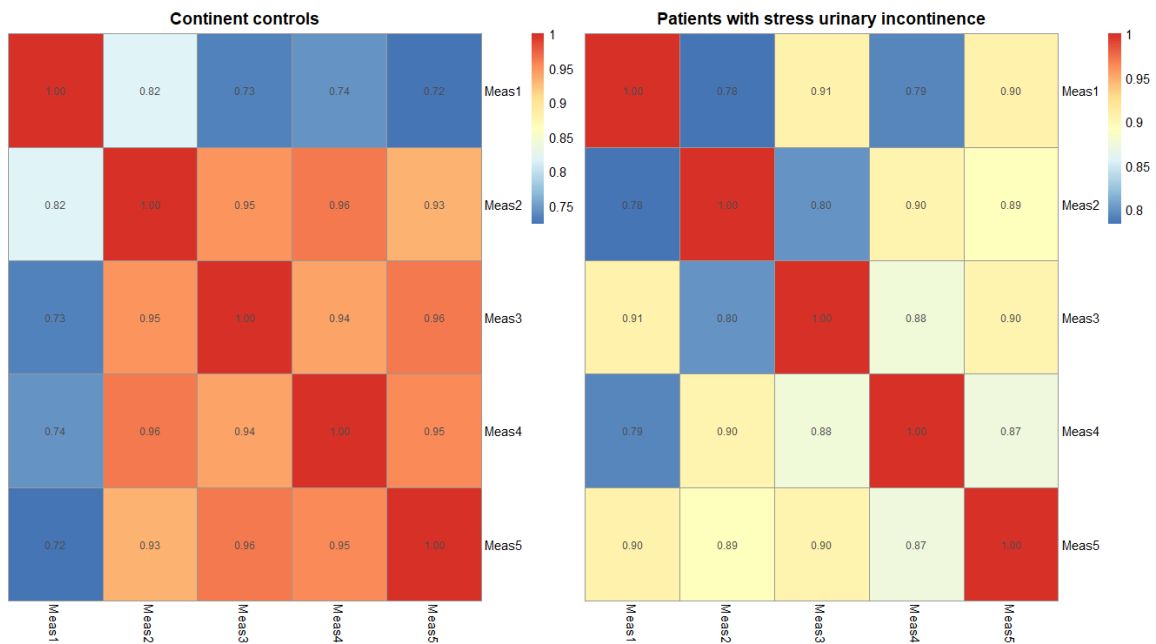


Figure S1. Intraclass correlation coefficients illustrating the repeatability of strain elastography measurements at the internal urethral orifice in continent controls and women with stress urinary incontinence.

Abbreviation: meas = measurement

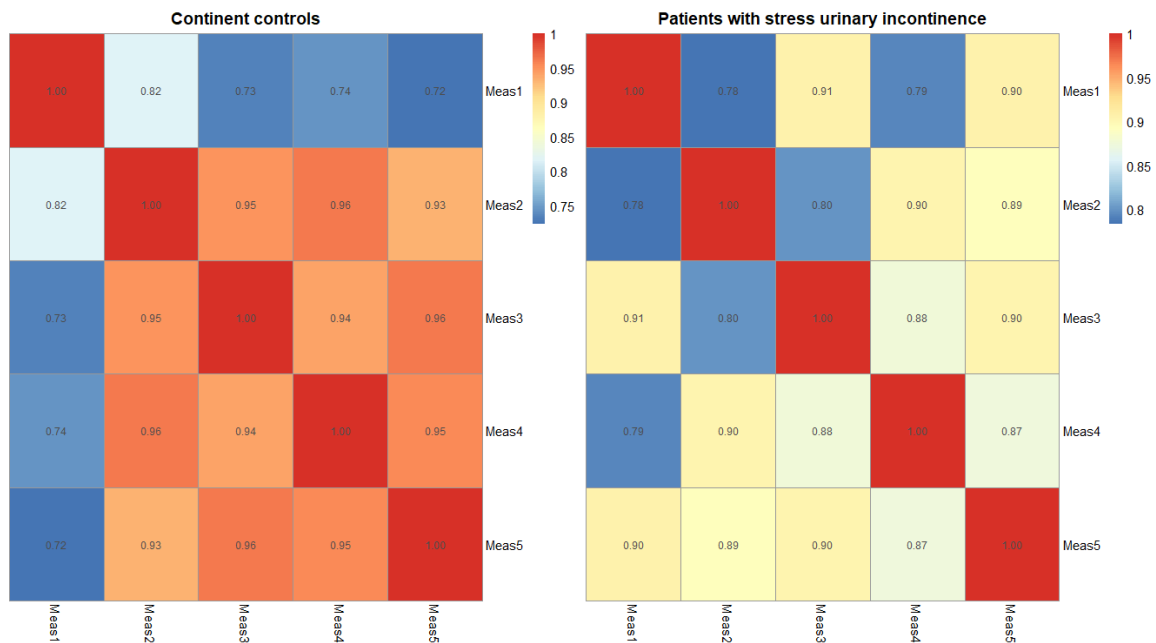


Figure S2. Intraclass correlation coefficients illustrating the repeatability of strain elastography measurements at the midurethral level in continent controls and women with stress urinary incontinence.

Abbreviation: meas = measurement

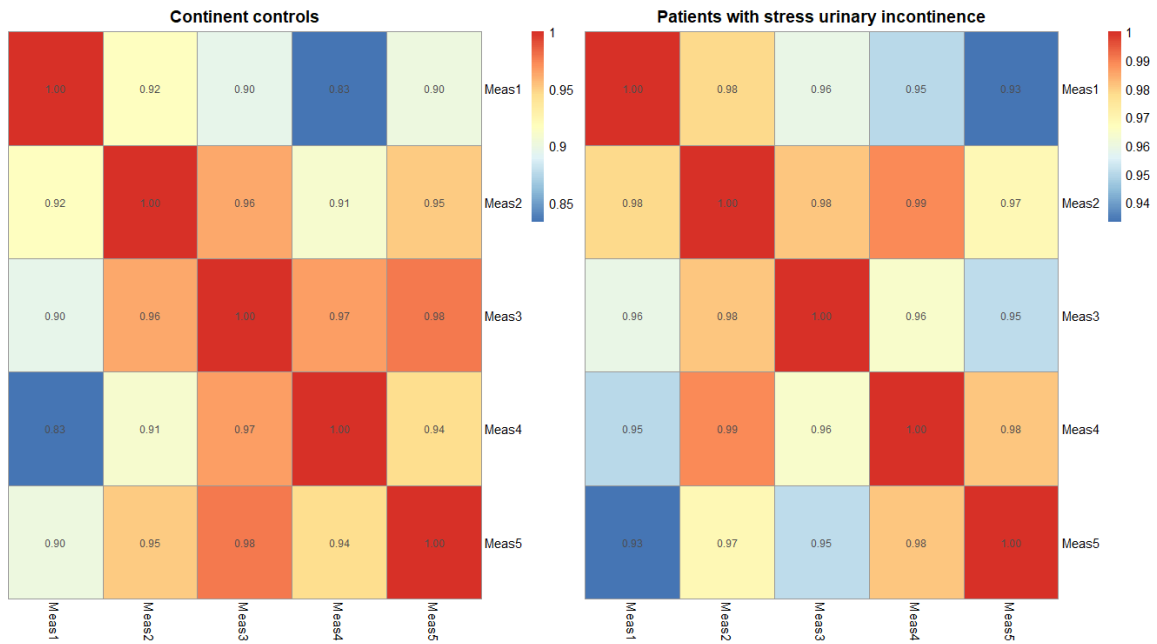


Figure S3. Intraclass correlation coefficients illustrating the repeatability of strain elastography measurements at the external urethral orifice level in continent controls and women with stress urinary incontinence.

Abbreviation: meas = measurement